ONLINE AND INTERACTIVE ENVIRONMENT FOR BIOSPECKLE LASER ANALYSIS BUILT IN JAVASCRIPT

Roberto Alves Braga Júnior*
Federal University of Lavras, Department of Automatica, Campus, ZIP Code 37.200-900, Lavras, MG, Brazil

Robson Pierangeli Godinho
RPG Software, ZIP Code 37.200-310, Lavras, MG, Brazil

*Corresponding author: robbraga@ufla.br

Abstract: The dynamic laser speckle, or biospeckle laser, is a reliable technique for monitoring activity in biological and non-biological material. The applications in agriculture are related to seed analysis, fruits maturity, identification of fungi, root growing among many other. However, despite the proved reliability as a sensitive, fast and objective sensor its adoption by new users demands computational knowledge, that in some cases presents as a limitation. Following a tendency of web-based solutions devoted to the dissemination of science, this work developed an online and interactive environment for analysing the BSL datasets by means of an accessible human-machine interface (HMI) using the JavaScript language, and adopting remote computing in the graphic cards of the users' computers. The environment was hosted by a web-site devoted to BSL and the results presented the feasibility of use developed tool in analysing all sort of BSL datasets. Particularly, in this work, the dataset of a coffee seed was analysed as an example.

Keywords: Cloud computing, dynamic laser speckle, web-based solution.

Received: February 14, 2025 - Accepted: March 24, 2025

INTRODUCTION

The laser speckle is an optical interference phenomenon that is observed when coherent light is scattered by a rough surface, presenting a chaotic, unordered, granular appearance (GOODMAN, 1975). When the dispersers of the light are not steady, changing in time, one can observe changes of the granular structure, and this temporal phenomenon is known as dynamic laser speckle, or bio-speckle laser (AIZU; ASAKURA, 1991). The bio-speckle, or biospeckle laser (BSL) is the dynamic laser speckle produced by biological material when illuminated. The information from the dynamic phenomenon can be linked to the level of activity in biological samples (XU; JOENATHAN; KHORANA, 1995), and the use of the phenomenon to measure the level of activity created a technique named after the biospeckle phenomenon. The application of the BSL technique can be widely observed in agriculture as presented by Zdunek et al. (2014), for example, with applications in fruits such as monitoring the ripening in tomatoes observed by Pavarin, Fracarolli, and Falcão (2024), or in the detection of fungi in citrus (YANG et al., 2024). In seed analysis one can see the BSL technique as a potential tool in vigor testing as presented by Xing et al. (2023), or even as a reliable test appointed by Braga, Contado, et al. (2025). The case of seed analysis was also used to develop and propose new approaches such as the Full Time History of the Speckle Pattern (FTHSP) presented by Puneet Thakur Singh et al. (2022), or the modified structural function (MSF) also presented by Puneet Singh et al. (2020). Despite the applications in fruits, seeds, root growing, animal sperm and many other practical cases in agriculture, the BSL demands effort to be accessible. The image processing can be mentioned as a first barrier to those who are not experts in computer science. Thus, the effort presented by Braga and Godinho (2023) in creating a web-based platform to facilitate the access to BSL datasets is a relevant contribution, based on the tendency

to use computing in the cloud. The environment Covira was presented by Ghimire et al. (2021) as a COVID-19 platform for risk assessment, visualization, and communication tool. It is an illustrative example of this effort to work using digital clouds for computing and sharing scientific information. In agriculture, the case of the AgDataBox API for the availability of key data in precision agriculture presented by Bazzi et al. (2019). In order to achieve better results in web-based platform, one can see the adoption of JavaScript language as presented by Mahmoudi et al. (2023) and by Kyriakou and Tselikas (2022). In addition, improvement in computer efficiency, particularly in image analysis, can be achieved by means of graphic cards (CHRISTIANSEN et al., 2021) as a storage of images. Advancements in utilizing graphics processing units (GPUs) have significantly enhanced image analysis across various domains. GPUs excel in parallel processing, making them ideal for handling the computational demands of image processing tasks (KIRIMTAT; KREJCAR, 2024). In this work, our objective was to create a web-based environment to assist new users and the experts in analyzing the speckle patterns in an interactive and online way, by means of Javascript language, and computing the data remotely and using the graphic cards.

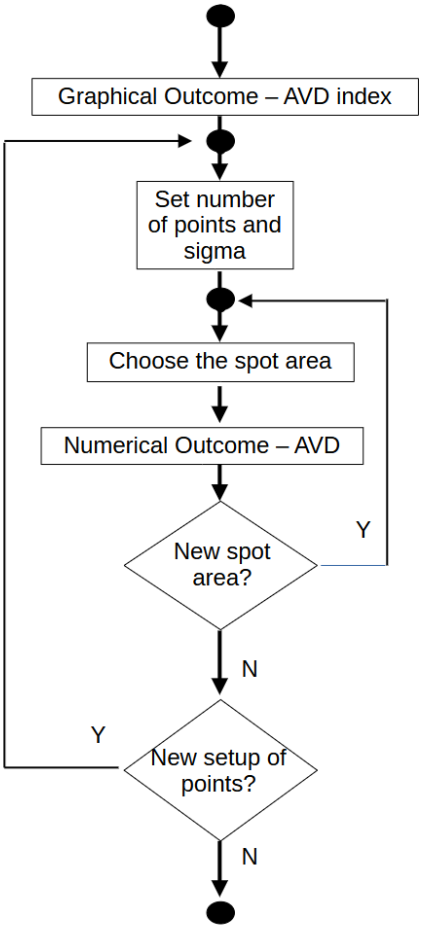

Figure 1: Flow of the two steps, graphical and numerical.

MATERIAL AND METHODS

Web environment and image processing

The online and interactive environment of biospeckle laser analysis was built within a web-page BSL on Clouds Braga and Godinho (2025a) using Javascript (https://bslonclouds.com).

The procedure was based on two steps: graphical and numerical, as presented in Figure 1. In the graphical outcome, one map of activity of a dataset of images to assist the user to choose the area of the sample will be numerically analysed. The graphical and numerical outcome was based in the BSL index known as Absolute Value of the Differences (AVD) (Equation 1).

$$AVD = \sum_{ij} \frac{COM(i,j)}{\sum_{lm} COM(l,m)} \mid i \; - \; j \mid \qquad (1)$$

Where COM is the co-occurrence matrix, and i, j, l and m are the lines and colunms of the COM matrix, varying from 1 to 256.

In the graphical outcome, the AVD index is obtained for each pixel in time, i.e. each pixel from the sequence of images. The final value is the level of gray. The low activity is, therefore, represented by 0 (black) and the high activity by 255 (white). The map of activity in gray scale is pseudo-colored varying from blue to red, representing black and white, respectively.

In the numerical outcome, the AVD index comes from the time history of the speckle pattern (THSP) matrix, that is built using a collection

https://doi.org/10.31422/taae.v9i2.66

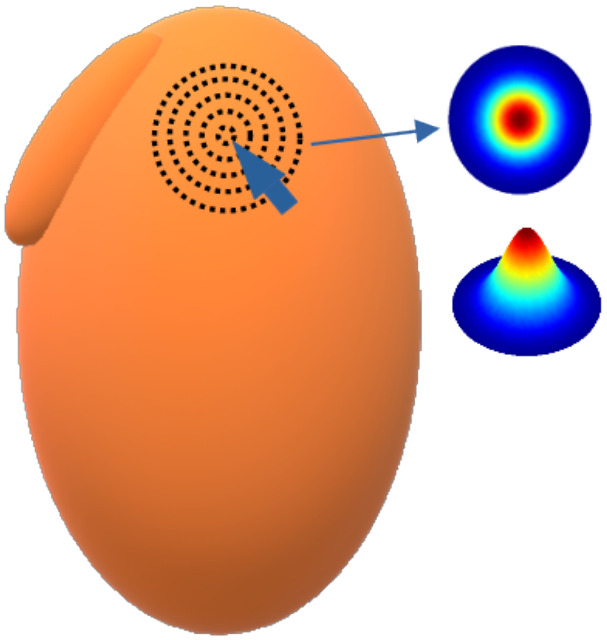

Figure 2: Illustrative seed with the circles representing the Gaussian area where the points will randomly be obtained, with the arrow representing the cursor of the mouse, selecting the central point of the Gaussian function.

of points from the speckle pattern image. The collection of points that can be obtained in the first image of the speckle pattern sequence can be from a line, from a Region of Interest (ROI) or even by a Gaussian distribution around the selected point by the user. We adopted the interactive solution provided by the selection of a point by the user moving the mouse over a graphic of the illuminated object. In Figure 2, an illustrative image of a seed can be seen with the traced rings presenting the cotes of the Gaussian distribution. The number of pints and the size of the Gaussian function (the standard deviation) is set by the user in an interactive way. The arrow represents the mouse over the image, pointing to the center of the area under analysis. In Figure 2, the representation of the Gaussian function is shown by dashed circles and by colored images in top view and 3D. The arrow points to the central spot area in the seed where the mean value (peak) of the Gaussian function is located. Therefore, it means that there are more points close to the peak, decreasing the number of points apart from the center. The dispersion of the points around the center is defined by the standard deviation (σ), therefore, the user can adjust the points restricted to the area under analysis. The colored representation of the Gaussian function defines that in the peak (mean value) in read the density (number) of points is higher than in the boundary.

Javascript codes

As shown in the flow of Figure 3, the images are collected by the system using the function *CollectImageData*, and then stored in RAM. These images, the speckle patterns, are matrices (bitmaps) that can be quite large and consume a significant amount of memory when processed using the computer's CPU and RAM.

To optimize the process, the *copyImageDataToCanvas* function transfers the images to the graphic processor (GPU) memory using the browser's *canvas* (from JavaScript language). Typically, the browser's *canvas* is processed by the computer's graphic card, allowing to shift the processing to the GPU, which, in most cases, is significantly faster than the central processor. The alternative processing enables real-time image analysis.

In code presented in Figure 3, we can also see the use of a pointer (*imgptr*), that addresses an array of images, to deal with the points that will construct the Time History of Speckle Pattern (THSP) reducing the image manipulation.

The THSP routine is presented in Figure 4, where the Gaussian points selected in the first speckle pattern are fixed and used to build the THSP matrix.

In the sequence, see the code in Figure 3, the calculus of the Co-occurrence Matrix (COM) is carried out. The COM is used to obtain the Absolute Value of the Differences (AVD) in the area selected in the illuminated object, presenting the biospeckle activity (BA).

The complete source of the codes can be found on GitHub (BRAGA; GODINHO, 2025b).

RESULTS AND DISCUSSION

The front page of the interactive and on-line tool is presented in Figure 5, where the user can access the activity map of the object that has been analyzed, in this case a coffee seed. The map of activity is the graphical outcome (Graphical AVD) of a sequence of only ten (10)

```
// Extract image data from speckle
// bitmaps
img_data = CollectImageData();

// Copy image data to image canvas
// These canvas are hardware treated
imgptr =
    copyImagesDataToCanvas(img_data);

// Get image points around clicked
// point - A Gaussian sample
area_gauss_points = getGaussian(x ,y);

// Calculate THSP matrix
THSP_matrix =
    calculateTHSP(area_gauss_points,
                              imgptr);

// Calculate COM Matrix: Co-occurrence
// matrix or co-occurrence matrices in
// gray level.
com_matrix = calculateCOM(THSP_matrix);

// Using COM Matrix to calculate AVD
AVD = calculateAVD(com_matrix);
```

Figure 3: Example of a code chunk with functions used in the Javascript code to get AVD from points.

```
calculateTHSP(area_gauss_points,
              img_ptr)
{
 gpoints = area_gauss_points.lenght;
 for (let idx = 0;
     idx < image_info_list.length;
     idx++)
 {
  let cvs_img = img_ptr[idx];
  for (let gauss_idx = 0;
      gauss_idx < gpoints;
      gauss_idx++)
 {
   let xvalue =
      area_gauss_points[gauss_idx].x;
   let yvalue =
      area_gauss_points[gauss_idx].y;
   let pix_val = getImagePixel(
      x + Math.round(xvalue),
      y + Math.round(yvalue),cvs_img);
   // THSP : image x gauss index
   THSP_matrix[gauss_idx][idx] =
        pix_val;
  }
 }
}
```

Figure 4: Code chunk with "calculateTHSP" function used in the Javascript code to get THSP matrix.

images of the speckle pattern in time. The low-resolution map of activity is used only as an orientation for the user to choose the area of the seed to be analyzed numerically. In Figure 5, one can also observe the result of the AVD index of the points, in a Gaussian distribution, used to obtain the THSP, in this case of a coffee seed obtained from the web-based environment BSL on Clouds (BRAGA; GODINHO, 2025a). The illumination of the selected points is presented in the histogram, which is relevant to evaluate if the observed area presents saturation or under exposition of laser light. In this case, 200 points, with a $\sigma = 10$, are placed in the embryo area of the seed.

When the user chooses another spot area in the seed, for example, outside of the embryo, the level of activity presented by the AVD index is lower (Figure 6). Therefore, the AVD index within the embryo is 23.75, when the points in the area other than the embryo present an activity of 17.52.

The user interactively moves the cloud of points

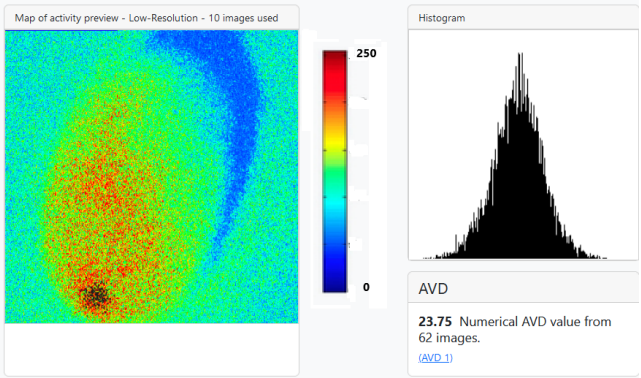

Figure 5: BSL online analysis of a coffee seed in the embryo area. The AVD index with the histogram.

over the map of activity and knows online the level of activity of the illuminated seed, always receiving the information of the quality of the illumination in the observer spot by means of the histogram.

This online and interactive solution for BSL processing is helpful in non-homogeneous samples, such as a seed; however, this web-based solution can be adopted in homogeneous samples.

https://doi.org/10.31422/taae.v9i2.66

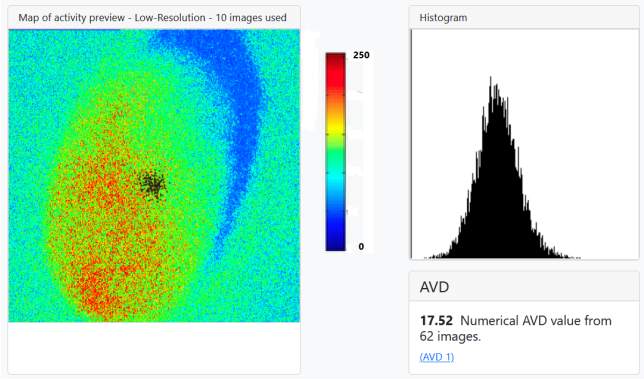

Figure 6: BSL online analysis of a coffee seed in an area aside of the embryo. The AVD index with the histogram.

The solution of running the analysis of images remotely in the users' computer was feasible and efficient in offering an online perception. The visual navigation on the screen helped the interactivity of the tool. The JavaScript presented a stable performance in the *BSL on Clouds*, and it has been a fundamental technology for developing web-based solutions. It enables interactivity, dynamic content updates, and real-time functionality, which makes it essential for modern web applications. JavaScript associated with CSS and HTML offers a visual interface for designing stimuli and allows customization (HENNINGER et al., 2022). The results of image processing with the cloud of points responsible for obtaining the numerical outcome are presented in Figure 5 and Figure 6, and it is the way users can save each attempt using the *print screen* function.

The web-based online solution presented in this work offers to the users the same experience obtained in traditional mathematical software as well as in stand-alone software, however, with the advantage of the interactive interface that eases the access by newcomers. The great difference though is the real-time sensation provided by the web-based solution. The limitation of the online solution is related to the fixed option made by the developers for the AVD1 index, while in the literature one can observe a multitude of numerical outcomes for quantifying the BSL phenomenon.

CONCLUSION

The online and interactive tool built using Javascript within and web-based environment to process BSL datasets by users presented reliability and ran in an online perception, allowing the users an easy navigation and with a visual control of the tasks. The graphical and numerical results were presented complementary with the aid of a histogram to check the quality of the speckle patterns.

ACKNOWLEDGEMENT

This work was supported by CNPq.

REFERENCES

AIZU, Y; ASAKURA, A. Bio-speckle phenomena and their application to the evaluation of blood flow. **Optics Laser Technology**, v. 23, n. 4, p. 205–219, 1991. DOI: 10.1016/0030-3992(91)90085-3.

BAZZI, Claudio L et al. AgDataBox API – Integration of data and software in precision agriculture. **SoftwareX**, v. 10, p. 100327, 2019. DOI: 10.1016/j.softx.2019.100327.

BRAGA, Roberto A; CONTADO, José Luís, et al. Analysis of Seed Vigor Using the Biospeckle Laser Technique. **AgriEngineering**, v. 7, n. 1, e3, 2025. DOI: 10.3390/agriengineering7010003.

BRAGA, Roberto A; GODINHO, Robson P. Biospeckle Laser On Clouds, a digital gateway aiming at collaborative research improvement. **Research Ideas and Outcomes**, v. 9, e114736, 2023. DOI: 10.3897/rio.9.e114736.

_____. **BSL on Clouds**. 2025. Available from: <https://www.bslonclouds.com>. Visited on: 31 Jan. 2025.

_____. **GitHub BSL on Clouds**. 2025. Available from: <https://github.com/robertobraga22/bslonclouds>. Visited on: 31 Jan. 2025.

CHRISTIANSEN, F et al. Ultrasound image analysis using deep neural networks for discriminating between benign and malignant ovarian tumors: comparison with expert subjective assessment. **Ultrasound in Obstetrics & Gynecology**, Wiley Online Library, v. 57, n. 1, p. 155–163, 2021. DOI: 10.1002/uog.23530.

GHIMIRE, Bhoj R et al. Covira: A COVID-19 risk assessment, visualization and communication tool. **SoftwareX**, v. 16, p. 100873, 2021. DOI: 10.1016/j.softx.2021.100873.

GOODMAN, Joseph W. **Statistical properties of laser speckle patterns**. 1. ed. Berlin Heidelberg: Springer, 1975. P. 9–75. Available from: <https://link.springer.com/chapter/10.1007/978-3-662-43205-1_2>.

HENNINGER, F et al. lab.js: A free, open, online study builder. Behav Res Methods, v. 54, n. 2, p. 556–573, 2022. DOI: 10.3758/s13428-019-01283-5.

KIRIMTAT, Ayca; KREJCAR, Ondrej. GPU-Based Parallel Processing Techniques for Enhanced Brain Magnetic Resonance Imaging Analysis: A Review of Recent Advances. **Sensors**, v. 24, n. 5, p. 1591, 2024. DOI: 10.3390/s24051591.

KYRIAKOU, Kyriakos-Ioannis D.; TSELIKAS, Nikolaos D. Complementing JavaScript in High-Performance Node.js and Web Applications with Rust and WebAssembly. **Electronics**, v. 11, n. 19, e3217, 2022. DOI: 10.3390/electronics11193217.

MAHMOUDI, Amin et al. OPA Solver: A web-based software for Ordinal Priority Approach in multiple criteria decision analysis using JavaScript. **SoftwareX**, v. 24, p. 101546, 2023. DOI: 10.1016/j.softx.2023.101546.

PAVARIN, Fernanda Fernandes Adimari; FRACAROLLI, Juliana Aparecida; FALCÃO, Alexandre Xavier. Biospeckle laser for assessing tomatoes ripeness indexes. **Revista Ciência Agronômica**, SciELO Brasil, v. 55, e20207677, 2024. DOI: 10.5935/1806-6690.20240022.

SINGH, Puneet et al. Application of laser biospeckle analysis for assessment of seed priming treatments. **Computers and Electronics in Agriculture**, v. 169, p. 105212, 2020. ISSN 0168-1699. DOI: 10.1016/j.compag.2020.105212.

SINGH, Puneet Thakur et al. Laser biospeckle technique for characterizing the impact of temperature and initial moisture content on seed germination. **Optics and Lasers in Engineering**, v. 153, p. 106999, 2022. DOI: 10.1016/j.optlaseng.2022.106999.

XING, Muye et al. Physiological Alterations and Nondestructive Test Methods of Crop Seed Vigor: A Comprehensive Review. **Agriculture**, v. 13, 2023. DOI: 10.3390/agriculture13030527.

XU, ZiJie; JOENATHAN, Charles; KHORANA, Brij M. Temporal and spatial properties of the time-varying speckles of botanical specimens. **Optical Engineering**, SPIE, v. 34, n. 5, p. 1487–1502, 1995. DOI: 10.1117/12.199878.

YANG, Si et al. Early detection of fungal infection in citrus using biospeckle imaging. **Computers and Electronics in Agriculture**, Elsevier, v. 225, p. 109293, 2024. DOI: 10.1016/j.compag.2024.109293.

ZDUNEK, Artur et al. The biospeckle method for the investigation of agricultural crops: A review. **Optics and Lasers in Engineering**, Elsevier, v. 52, p. 276–285, 2014. DOI: 10.1016/j.optlaseng.2013.06.017.